Laser and Particle Beams (1999), *vol.* 17, *no.* 2, *pp.* 265–273
Printed in the United States of America

Problems of measurement of dense plasma heating in laser shock-wave compression

By D. BATANI,* M. KOENIG,** A. BENUZZI,** I.K. KRASYUK,† P.P. PASHININ,† A.Yu. SEMENOV,† I.V. LOMONOSOV,†† AND V.E. FORTOV††

*Universitá degli Studi di Milano, Dipartimento di Fisica, Via Emanueli, 20146 Milano, Italy
**LULI, Ecole Polytechnique, 91128 Palaiseau, France
†General Physics Institute of the Russian Academy of Sciences, 38 Vavilov Street, Moscow 117942, Russia
††High Energy Density Research Center of the Russian Academy of Sciences, 13/19 Izhorskaya Street, Moscow 127412, Russia

(Received 5 July 1998; Accepted 2 December 1998)

Experimental results of heating measurements of matter carried out in a study of laser-driven shock waves in aluminum (Batani *et al.* 1997) are discussed. The measured temporal evolution of the "color" temperature of the rear surface of the target is compared with that computed by a numerical code. It has been established that the target preheating can substantially affect optical signal features recorded from the rear side of the target, and consequently influence upon the accuracy of temperature and pressure measurements of the material behind the shock wave front.

1. Introduction

Application of dynamic methods of diagnostics for investigation of thermodynamic properties of matter in a wide range of parameters supposes stationarity and one-dimensionality of hydrodynamic flows as well as definition of initial conditions for a target material in front of the shock wave. Initial conditions of the target plays a significant role since the laser-driven shock-wave generation is associated with formation of a high-temperature plasma, which may cause target preheating by X rays and fast electrons. Temperature measurements of the shock-heated plasma in metals is a complicated problem mainly due to screening of radiation—emerging from hot target regions—by cooled vapors of the material released by the rarefaction wave which follows the shock breakout at the target–vacuum boundary (Zel'dovich & Raizer 1967).

2. Experimental details

In the experiment, laser radiation at 0.53 μm was used with the intensity onto the target up to 3×10^{13} W/cm^2 with the Gaussian pulse duration $\approx$ 600 ps (full width at half measure, FWHM) (Batani *et al.* 1997). A special "smoothening" technique was applied to obtain a flat profile of intensity distribution over the focal spot of 200 μm in diameter (Koenig *et al.* 1994). The two-stepped aluminum targets with a base thickness of 9.4 μm and the step height h_s of 4μm were used. The choice of material was caused by the fact that the equation of state (EOS) for aluminum is well known.

To determine "color" temperature of the material in the rarefaction wave, a two-channel pyrometer was used. The pyrometer recorded luminosity from the rear surface of the target in the "red" (0.6 μm) and "blue" (0.4 μm) spectral ranges, respectively. The relevant optics

© 1999 Cambridge University Press 0263-0346/99 $12.50

included a biprism and two spectral filters. A streak camera provided 5-ps resolution for the light emission recorded from the rear surface of the target.

3. Numerical modelling

To define the shock-wave characteristics on the basis of experimental data, a 1D numerical code was specially developed (Semenov 1997). The computational model employed hydrodynamic equations in the Lagrangian variables to which the thermodynamically complete wide-ranging semiempirical multiphase EOS for aluminum was added (Bushman & Fortov 1983). To compute the temporal behavior of the luminous radiation temperature of the material in the rarefaction wave, we applied the approach Zel'dovich and Raizer (1967), based on calculation of spectral brightness of the emitting layer with known spatial density and temperature distributions shown schematically in figure 1b.

The intensity of the radiation at a wavelength λ emitted at time t by the material at position x with temperature $T(x,t)$ is given by

$$B_\lambda = \int_0^d B_\lambda^0[T(x,t)] \exp\left[-\int_0^x \tilde{\chi}_\lambda(\xi,t)\,d\xi\right] \tilde{\chi}_\lambda(x,t)\,dx, \tag{1}$$

where d is the target–vacuum boundary,

$$B_\lambda^0 = \frac{2hc^2}{\lambda^5} \frac{1}{\exp(hc/\lambda\, kT) - 1}$$

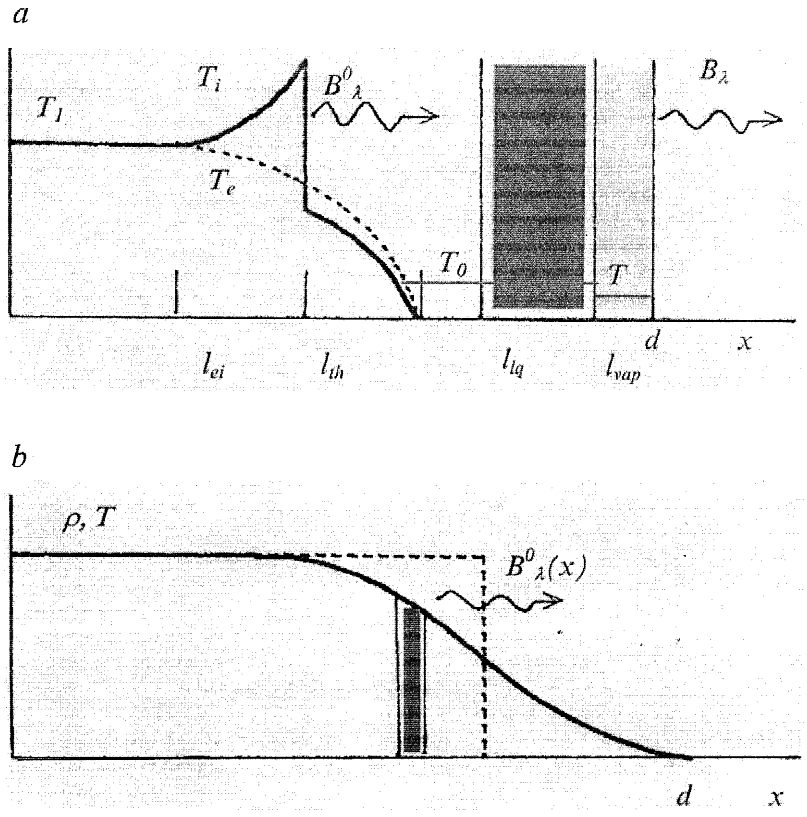

FIGURE 1. Schemes of the shock-wave front structure (a) and of the released profiles of mass density $\rho(x)$ and temperature $T(x)$ (b).

is the spectral brightness of the black-body radiation,

$$\tilde{\chi}_\lambda(x,t) = \chi_\lambda(x,t)\{1 - \exp[-hc/\lambda\, kT(x,t)]\}$$

is the material opacity with the induced emission taken into account.

The effective "color" temperature T was deduced from the relation:

$$\left(\int_{\Delta\lambda_{red}} B_\lambda\, d\lambda\right)\Big/\left(\int_{\Delta\lambda_{blue}} B_\lambda\, d\lambda\right) = \left(\int_{\Delta\lambda_{red}} B^0_\lambda\, d\lambda\right)\Big/\left(\int_{\Delta\lambda_{blue}} B^0_\lambda\, d\lambda\right) = K(T), \qquad (2)$$

where $\Delta\lambda_{red}$ and $\Delta\lambda_{blue}$ are the "red" and "blue" spectral bands of the pyrometer (see figure 2b).

For computing the temporal history of the "color" temperature of the rear surface, the spatial profiles of density ρ and temperature T at different times during the shock-unloading process were calculated. The calculations were made with a spatial resolution of <0.05 μm and with a temporal resolution better than 8 ps.

The opacity χ_λ was calculated in two ways (Semenov 1995): with the help of Kramers–Unsold formula and by means of a numerical code based on using generalized "chemical" models with nonideal effects, degeneracy, and metal-dielectric transition taken into account. In the code after finding plasma composition, the absorption coefficient was computed by a summation of contributions to photoionization over all channels, the inverse bremstrahlung absorption in the field of ions being added. The absorption in cold metal was taken into account by a semiempirical model.

4. Processing of the experimental data

Shown in figure 3 are photochronograms of luminescence for the "red" and "blue" spectral ranges recorded in the experiment Batani *et al.* (1997), and the result of their fitting by the least-square method.

The "color" temperature was determined from the temperature dependence of intensity ratio of the black-body radiation for the "red" and "blue" spectral ranges using the expression for $K(T)$ (see figure 2a). The spectral sensitivity of each channel was taken into account. The observed temporal history of the rear surface "color" temperature is shown by thick lines in figure 4. The temperature rise time at the base ($t_b = 52.5$ ps) and the temperature amplitude proved to be higher than those at the step ($t_s = 33.5$ ps). The leading edge of one of the curves reveals a kind of a pedestal which is a preheating feature, the target preheating temperature being $0.45^{+0.15}_{-0.06}$ eV.

5. The results of numerical modelling

5.1. *Calculation of the ablation and shock-wave pressure*

The ablation pressure amplitude P_0 on the target surface wave was defined by computer modelling of the measured time needed for the shock front to travel the base distance equal to the step height of the target. In the procedure, the pattern of the pressure pulse at the target surface was supposed to repeat the Gaussian shape of the laser pulse. Computation showed that the delay of the optical signal escaping the step is equal to the measured one ($t_s = 203$ ps) at $P_0 = 6.8$ Mbar. The shock-wave pressure along the base distance $P_s = 6.5$ Mbar has been computed. Assumption of the stationary state allows one to find the shock speed D which is equal to $h_s/t_s = 19.7$ km/s. The shock-wave adiabatic curve table gives $P_{st} = 6$ Mbar. The difference between P_s and P_{st} indicates some deviation of the shock-wave generation process from the stationary one under the experimental conditions.

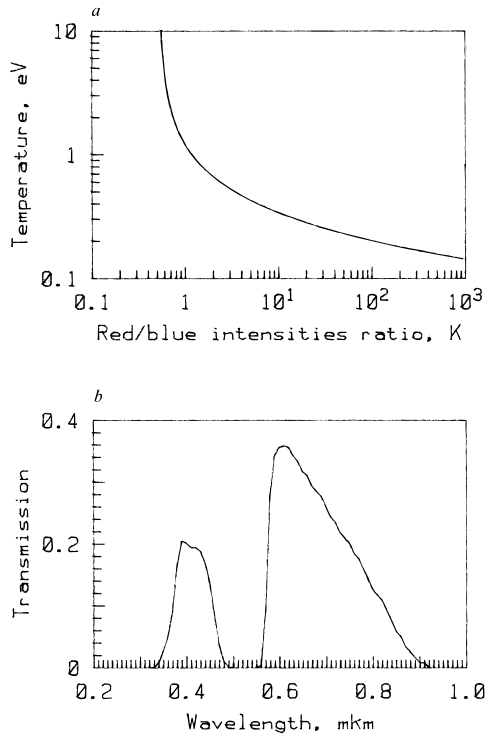

FIGURE 2. The two-channel pyrometer characteristics. The curve (a) is a result of calculation based on relation (2). On figure (b) the spectral bands of pyrometer are shown.

5.2. *Calculation of the temporal evolution of the "color" temperature*

To determine the "observed" temperature of the rear target surface, the release spatial profiles of density and temperature by rarefaction wave were found at subsequent time moments. After that, using expressions (1), (2), and the curve in figure 2a, the temporal history of the "color" rear surface temperature was calculated (figure 4). It is obvious that application of different models for calculation of the opacity of aluminum gives rise to close results, the absorption found on the basis of Kramers–Unsold model being slightly larger. Also shown in figure 4 are calculations of the temporal evolution of the maximal true temperatures in the course of the shock-unloading material at the respective surfaces of the target. Figure 4 clearly shows that measurement of the true temperature of the shock-heated aluminum would require a temporal resolution better than a few picoseconds.

5.3. *The shock-wave structure and rise time of the optical signal in case of cold metal*

The structure of shock wave front (Zel'dovich & Raizer 1967) is shown schematically in figure 1a. In a strong shock, a sharp difference in ion and electron temperatures arises: ion temperature exceeds the electron one considerably. Since the intensity of optical emission is related mainly to the electron temperature, the growth of recorded light signal depends on an electron–ion relaxation time. Estimates made in Zel'dovich and Raizer (1967) give $l_{ei} = 4 \times 10^{-6} \div 3 \times 10^{-4}$ μm for the width of the relaxation zone—where electron and ion temperatures become equal. If electron thermal conductivity is taken into consideration, then the heated zone before the shock wave front can be estimated by Zel'dovich and Raizer (1967) as

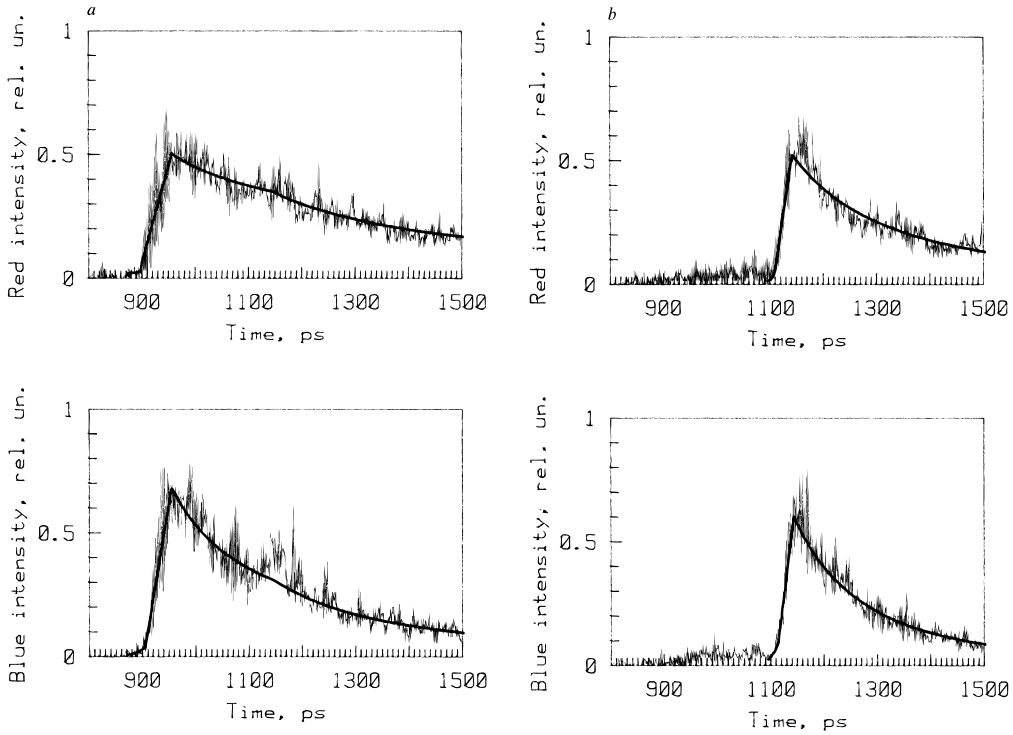

FIGURE 3. The observed "red" and "blue" light emission on a rear side of the target. (a) base surface; and (b) step surface.

$l_{th} = (2/5)\chi_e/D = 2 \times 10^{-5} \div 5 \times 10^{-3}$ μm (χ_e is the coefficient of electron temperature conductivity).

Thus, in an aluminum target being initially at normal conditions of $T = 293$ K and $\rho = 2.7$ g/cm^3 the full width of the shock wave front does not exceed $l_{ei} + l_{th} \approx 6 \times 10^{-3}$ μm. Hence, the rise time of recorded optical signals being equal to $t_1 \approx (l_{ei} + l_{th} + l_{opt})/D$ does not exceed 1 ps in case of normal state of the target. The value of l_{opt} is given by formula:

$$\tau_{opt} = \int_{d-l_{opt}}^{d} \tilde{\chi}(x)\, dx \approx 1.$$

Here τ_{opt}, $\tilde{\chi}$, and d are the optical depth, the opacity, and the target–vacuum boundary location, respectively. In case of cold aluminum layer width l_{opt} is roughly equal to 10^{-2} μm.

5.4. *Preheating and its action on light signals and target characteristics*

In this section, the results of numerical modelling of the luminous radiation emitted by the rear surface of the preheated planar target with thickness of 9.4 μm are presented. It was suggested that heating is caused by uniformly distributed over the volume heat sources of constant power 1.7×10^{13} W/cm^3. This value of power leads to the expected value of matter heating before shock wave front: 0.3–1 eV (Honrubia *et al.* 1997). Other conditions were in accordance with those held in experiment by Batani *et al.* (1997). At first the released profiles of mass density and temperature in the unloading material were calculated with preheating of the target taken into account. Then, the temporal evolution of the light emission temperature was calculated using relations (1) and (2). The results are shown in figure 5b. In this case, the

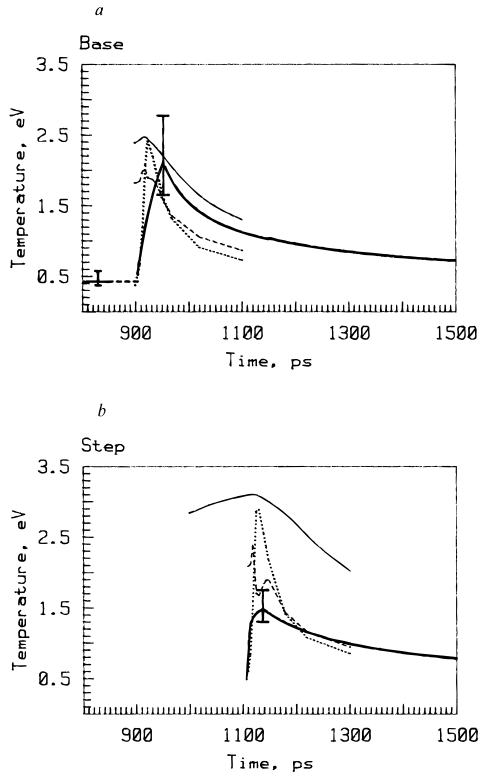

FIGURE 4. The measured and calculated temporal evolution of the temperature. (a) base surface; and (b) step surface. Solid thick line—the experimental results; solid thick line—the calculated maximum values of the target true temperature; dotted line—the semiempirical model for the opacity calculation; and dash line—the Kramers–Unsold formula for the opacity.

calculated rise time of the temperature $t_2 = 22.5$ ps turned out to be comparable with the recorded value.

The calculations showed that the metal at the rear target's side expands isothermally at temperature $T_0 = 5200$ K (0.45 eV) with delay of time $t_0 = 0.5$ ns relatively at the beginning of the process. In consequence of the preheating process, the expansion velocity is equal to $u_{exp} = 2.2$ km/s and the target–vacuum boundary shift is approximately equal to 1 μm. The arrows on figure 6 show the original position of the target–vacuum boundary. The step height will be enlarged by value $\delta h_s = u_{exp} t_s \cong 0.5$ μm. The material in rarefaction wave comes into a region of two-phase state after transit through solid and liquid states.

5.5. *Evolution of the gas-phase material properties at the liquid–vacuum interface*

For the evaluation of features of evaporated matter in the gas phase, analytical estimates were performed on the base of models developed in Anisimov *et al.* (1970). Atomic density in saturated vapor n_0 [cm^{-3}] as a function of surface temperature T_0 [eV] is defined by the following semitheoretical expression:

$$n_0 = \frac{A}{T_0^{3/2}} \exp\left(-\frac{B}{T_0}\right). \tag{3}$$

In this expression, $A = 2.47 \times 10^{23}$ and $B = 3.08$. At $T_0 = 0.45$ eV, formula (3) gives $n_0 = 8.5 \times 10^{20}$ cm^{-3}. Formation of the gas dynamic flow of steam arises at a distance $l = 1/\sigma\, n_0 = 1.8 \times$

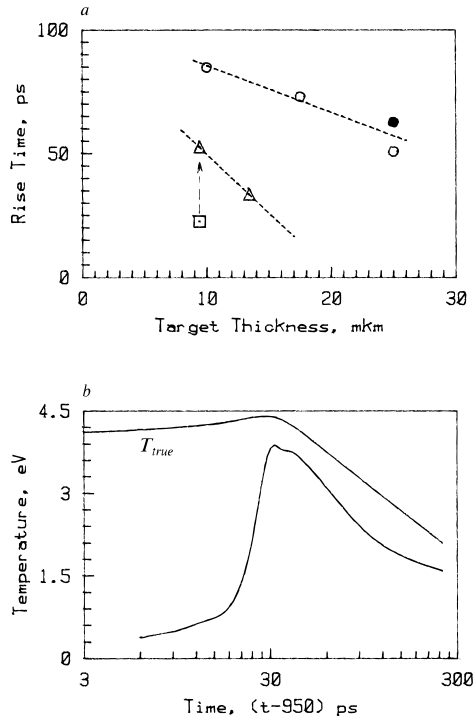

FIGURE 5. The experimental light emission characteristics (rise time of an optical signal on the target rear surface as a function of the target thickness). (a) laser (Δ) and X ray (○,●) driven shock wave: Δ—Batani *et al.* (1997); ○—Lower *et al.* (1994), ●—Evans *et al.* (1996); and □—this work results. The calculated "observed" temperature evolution in case of preheating (b). The upper line is the maximum true temperature of the shock heated target.

10^{-6} cm, where σ is the gas-kinetic cross section for aluminum atoms. Density and temperature values of evaporated material in the hydrodynamic flow turn out to be equal: $n = 0.31n_0 = 2.6 \times 10^{20}$ cm^{-3}, and $T = 0.65T_0 = 0.3$ eV. The velocity of gas dynamic expansion reaches 1.2 km/s relatively to the heated surface. The evaluations show that by the moment of shock wave release an evaporated cloud occupies region with length $l_{vap} = 0.54$ μm and has optical density τ_{opt}, approximately equal to 0.25. This layer contributes $t_3 \approx l_{vap}/D \approx 27$ ps in increase of the rise time of the optical signal. Thus, the overall rise time of the "observed" optical emission can be evaluated as $t_{sum} \approx t_1 + t_2 + t_3 \approx 50$ ps in case of the target preheating.

Thereby, the results of numerical calculations and analytical evaluations show that preheating process leads to formation on the free targets surfaces the layer of matter in mixed liquid–gas state of full thickness $l_{sum} = 1.5$ μm, where the density is varied from 2.7 cm^{-3} to 1.2×10^{-2} cm^{-3}. This layer absorbs light and leads to a drop of optical signal amplitude and to distortion of true temperature measurements. In this case, the value of rise time for the calculated luminous radiation emitted by the surface may exceed tens of picoseconds. Estimations show that electron-ion relaxation time varies from 1 fs to 15 ps (at the vapor–vacuum boundary with vacuum) in this layer that leads also to elongation of the observed optical signal rise time.

6. CONCLUSION

To interpret the laser shock-wave experiments correctly, it is necessary to take into account the possibility of change of matter state on the free surface of the target in front of the shock. The existence of this layer with changed properties can essentially affect the moment of ap-

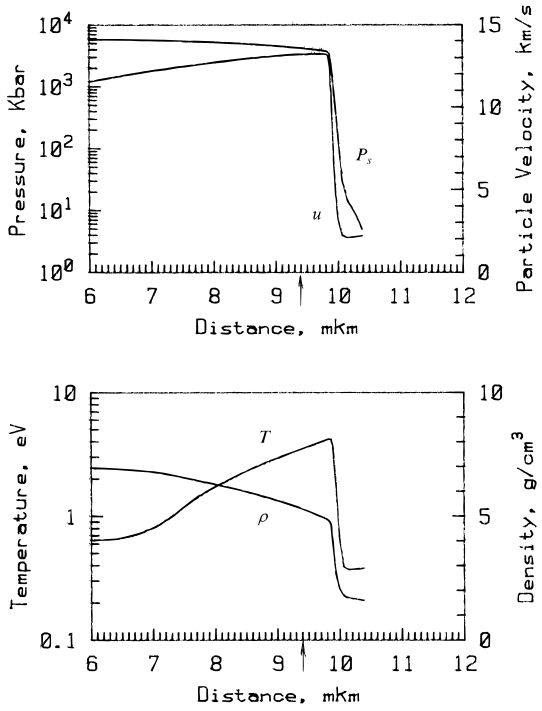

FIGURE 6. The spatial shock-wave characteristics in case of preheating in the time moment before shock-wave arrival at the target–vacuum interface. The arrows show the original position of the target–vacuum boundary.

pearance and the shape of the "observed" optical signals recorded from the rear surface of the target. Hence, to determine the true pressure and temperature in laser shock-wave experiments, based on measurements of recorded luminous radiation emitted by the rear surface, some inadmissible errors may appear.

Since the light emission brightness of the heated layer strongly depends on temperature, it is difficult to distinguish at one laser shot optical signals from the preheated metal and those from the heated shock. To measure the preheating temperature one has to use a two-foil target with a step-to-base spacing equal to 20…30 μm. Such a target design will not practically change the conditions of target preheating for the corresponding step while the moment of appearance of bright light emission caused by the shock of compressed matter will be delayed by a value equal to 1…1.5 ns. As a result the sensitivity of recording weak light emission, associated with the preheating, can be increased at the expense of the decrease of temporal resolution.

Acknowledgments

Authors would like to thank Dr. A.A. Charakhch'an and Dr. E.I. Shklovski for their comments which helped to improve this paper. This work has been supported by INTAS-RFBR Grant 95-0631.

REFERENCES

ANISIMOV, S.I. *et al.* 1970 *Effects of High-Power Radiation on Metal* (Nauka, Moscow, USSR).

BATANI, D. *et al.* 1997 *Advances in Laser Interaction with Matter and Inertial Fusion* (ECLIM'96, Madrid, Spain), p. 409.

BUSHMAN, A.V. & FORTOV, V.E. 1983 *Usp. Fiz. Nauk.* **140**, 177. [1983. *Sov. Phys. Usp.* **26**, 465].

EVANS, A.M. *et al.* 1996 *Laser Particle Beams* **14**(2), 113.

HONRUBIA, J.J. *et al.* 1997 *Advances in Laser Interaction with Matter and Inertial Fusion* (ECLIM'96, Madrid, Spain), p. 34.

KOENIG, M. *et al.* 1994 *Phys. Rev. E* **50**(5), R3314.

LOWER, TH. *et al.* 1994 *Phys. Rev. Lett.* **72**(20), 3186.

SEMENOV, A.YU. 1995 In *Laser Interaction and Related Plasma Phenomena, 12 Int. Conf.* Osaka, Japan, April 1995. S. Nakai and G.H. Miley, eds. Amer. Inst. of Physics, AIP Conference Proc. **369**, Part one (Woodbury, New York). p. 434.

SEMENOV, A.YU. 1997 *Comp. Maths Math. Phys.* **37**(11), 1334.

ZEL'DOVICH, YA.B. & RAIZER, YU.P. 1967 *Physics of Shock Waves and High Temperature Hydrodynamic Phenomena* (Academic Press, New York).